International Journal of Mechanical, Industrial and Aerospace Sciences
ISSN: 2517-9950
Vol:8, No:1, 2014

Application of Digital Image Correlation Technique on Vacuum Assisted Resin Transfer Molding Process and Performance Evaluation of the Produced Materials

Dingding Chen, Kazuo Arakawa, Masakazu Uchino, Changheng Xu

***Abstract*—**Vacuum assisted resin transfer moulding (VARTM) is a promising manufacture process for making large and complex fiber reinforced composite structures. However, the complexity of the flow of the resin in the infusion stage usually leads to nonuniform property distribution of the produced composite part. In order to control the flow of the resin, the situation of flow should be mastered. For the safety of the usage of the produced composite in practice, the understanding of the property distribution is essential. In this paper, we did some trials on monitoring the resin infusion stage and evaluation for the fiber volume fraction distribution of the VARTM produced composite using the digital image correlation methods. The results showthat3D-DIC is valid on monitoring the resin infusion stage and it is possible to use 2D-DIC to estimate the distribution of the fiber volume fraction on a FRP plate.

***Keywords*—**Digital image correlation, VARTM, FRP, fiber volume fraction.

I. Introduction

VACUUM assisted resin transfer moulding (VARTM) is widely used for moulding of complicated composite structures because of its ease of operation and low cost, and has been applied to marine vessels and next generation airplanes[1]. However, compared with the other typical manufacturing process, VARTM is young and meets many problems, such as low fibre volume fraction and nonuiform property distributions of its products. Consequently, amount of works have been performed to improve this process and try to get a deeper understanding of it.

In order to improve the quality of the VARTM produced composite parts, a large amount of researches were done to improve this process[2]-[7]. Almost all of these improvements aimed at realizing a uniform flow of the resin in the resin infusion stage. Consequently, a comprehensive understanding of the flow is essential. The Center for Composite Materials in University of Delaware has a series research on VARTM [8]-[11]. Simacek[10] built a theoretical mold to simulate the flow of the resin. This mold was then proof to be valid by his experiments[11]. Almost at the same time, a research group in the University of Auckland finished the similar research [12]-[14]. And, in their research, they developed a digital speckle stereophotogrammetry system which is a full-field test system to monitor the thickness evolution of the package [13]. Both of their researches show that thickness of the stack is an important parameter to response the infusion of the resin.

On the other hand, the property distributions of VARTM produced materials usually are not uniform. Since the distribution is not uniform, it is essential to estimate the distribution for the safe use. Fiber volume fraction is one of the most important properties of composite materials. There are two standard methods testing this parameter[15]. One is removing the matrix componentby using a hot liquid medium[16] or a furnace[17]. The operation of this method is a little complex. The most important is this method need destroy the material. The other is a calculation with the thickness of the composite material and the density of the reinforcement components. However, the composite part made by VARTM process usually only has one smooth surface, making it difficult to measure the thickness accurately. Consequently, if there is a nondestructive method which can estimate the fiber volume fraction, or even giving a rough distribution, it would be very useful for the safe use of VARTM manufactured composite materials.

In this paper, we did some trials on monitoring the resin infusion stage in VARTM process and evaluation for the distribution of the fiber volume fraction of the VARTM produced CFRP plate using the digital image correlation methods. A three dimensional digital correlation method (3D-DIC) technique was adopted to research the resin infusion process by monitoring the thickness evolution of the stack of fabrics. A two dimensional digital image correlation technique (2D-DIC) was used to calculate the coefficient of thermal expansion (CTE) which is related to the fiber volume fraction to estimate the distribution of the fiber volume fraction.

II. Digital Image Correlation Method

A. 2D-DIC

The sketch of 2D-DIC method is shown in Fig. 1. This

Dingding Chen is with the Interdisciplinary Graduate School of Engineering Science, Kyushu University, Fukuoka, CO 816-8580 Japan (e-mail: dingding.mail@163.com).

Kazuo Arakawa is with the Research Institute for Applied Mechanics, Kyushu University, Fukuoka, CO 816-8580 Japan (phone: 81-92-583-7761; fax: 81-92-593-3947;e-mail: k.arakaw@riam.kyushu-u.ac.jp).

Masakazu Uchino is with the Mechanic & Electronics Research Institute, Fukuoka Industrial Technology Center, Kitakyusyu, CO 807-0831 Japan (e-mail: muchino@fitc.pref.fukuoka.jp).

Changheng Xu is with the Interdisciplinary Graduate School of Engineering Science, Kyushu University, Fukuoka, CO 816-8580 Japan (e-mail: xuchannhenn@yahoo.co.jp).

method recognizes the same point in two pictures taken before and after deformation of an object through some correlation equations. And then it compares the positions of the point in the two pictures to get the displacement [18] .A small subset ($N\times M$) centered at a pixel point $P(X,Y)$ on the undeformed object image is used to obtain an estimate of the displacement of a point P. Intensity values of all points in the subsets ($N\times M$) on the undeformed image are compared to the intensity values of other subsets on the deformed image by using the following equation,

$$C(X+u,Y+v)=\sum_{i=-M}^{M}\sum_{j=-M}^{M}\left|I_d(X+u+i,Y+v+j)-I_u(X+u,Y+v)\right| \quad (1)$$

where $N=2M+1$, C is a correlation function. I_d and I_u are intensity values of a point on the deformed and undeformed images, respectively. The values, u and v, are displacement components in the x and y directions, respectively. The values of u' and v' which minimize C are roughly assumed to be the displacements in pixel. The precision of the result is only 1 pixel. With some further analysis [19], a better precision higher than 1 pixel can be calculated. Then with the relationship between the pixel and the real length, the displacement with a high precision can be obtained.

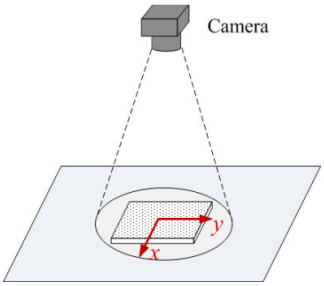

Fig. 1 Sketch of 2D-DIC method

B. 3D-DIC

In 3D-DIC system, two cameras focusing at the same location are used to measure the spatial displacement of a object as shown in Fig. 2. A spatial coordinate (X, Y, Z) for the object and two plane coordinates (U, V) on the camera CCD surface are built. A displacement of the object, (x, y, z), in the spatial coordinate system will cause a displacement on the two camera coordinates, (u_1, v_1) and (u_2, v_2), which can be calculated using the method introduced in the last part. Referring to [20], [21], when the displacement is small, u_i and v_i (i=1 and 2) can be considered as an overlap of three independent effects caused by x, y and z respectively, expressed by

$$\begin{aligned} u_i &= f_{uxi}(x)+f_{uyi}(y)+f_{uzi}(z) \\ v_i &= f_{vxi}(x)+f_{vyi}(y)+f_{vzi}(z) \end{aligned} \quad ,i=1 \text{ and } 2 \quad (2)$$

In the right side, the expressions, f, are quadratic equations about x, y and z, respectively. With some calibration work, the detailed expression of f can be fixed; thereby the expressions (2) can be fixed. Then, in the test, the displacement of an object, (x', y', z'), in the spatial space can be calculated by solving the equation set (2) with the displacements, (u_1', v_1') and (u_2', v_2'), recorded by the cameras.

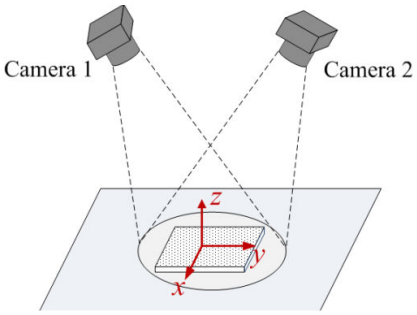

Fig. 2 Sketch of 3D-DIC method

III. Monitor of Resin Infusion Process

A. Experiment

Fig. 3 is a schematic diagram of the VARTM process and the 3D DIC test system. Eight layers of a [30°/–30°] stitched carbon fiber fabric (Saertex GmbH & Co. KG) were laid on a solid mold and covered with a peel ply. The inlet and the vent, located on either side of the stack, were made using a rubber connecter and a segment of a spiral tube, forming a linear inlet (and vent), and thereby provided uniform resin flow. The entire structure was then enclosed in a transparent vacuum bag and sealed with tape. The resin (XNR/XNH6815, Nagase & Co., Ltd.) was infused after drawing a vacuum. The inlet was closed once the resin reached the vent and began to flow out of the package. The vent was left open for about another 30 min to extrude the excess resin from the package. The size of the stack was 170 × 140 mm. Two bands having random patterns were made on the transparent vacuum bag for DIC analysis (Fig. 3 (b)). The other parts were left unpainted to observe the flow inside the package. Two cameras were focused on the same area and were computer-controlled so that they would record images simultaneously. The entire infusion process was recorded. The precision of the 3D-DIC test system could reach 0.01 mm.

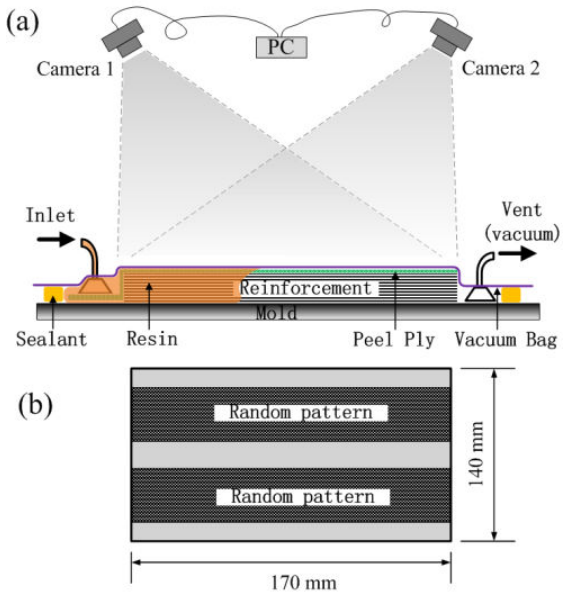

Fig. 3 (a) Schematic diagram of the VARTM process with the thickness monitoring system. (b) Top view

B. Results and Discussion

Fig. 4 shows the vacuum package and the full-field thickness change distribution at 17 min. The time was counted from the time of opening the inlet. The resin was infused from the left side. The stack of fabric changes from gray to black due to the saturation of the resin. Consequently, the outline of the black area in Fig. 4 (a) shows the flow front of the resin. Fig. 4 (b) is the full-field thickness change distribution of the package. Fig. 4 (c) shows the thickness change distribution along the line from point *A* to point *E* marked in Fig. 4 (a). Fig. 5 shows the thickness evolution of the five points, from *A* to *E* shown in Fig. 4 (a), on the vacuum package. Fig. 5 shows, after opening the inlet, point *A* expanded quickly due to a mass of the resin was infused. However, the other points, from *B* to *E*, had an obvious shrinkage stage. These parts shrank first and then expanded. Simacek [11] and Yenilmez [22], [23] also found the similar phenomenon in their researches. After closing the inlet at about 50 min, the entire part began to shrink together, because no resin was infused anymore, but extra resin was continue to be extruded until the vent was closed. After closing the vent at about 80 min, the thickness still decreased a little, showing a creep like property [24].

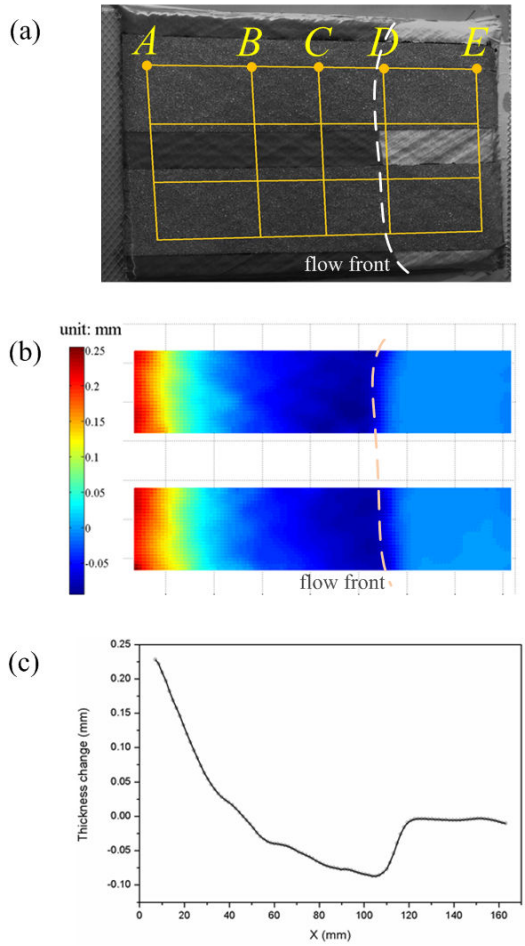

Fig. 4 (a) Photograph of the vacuum package.(b) Full-field thickness change distribution. (c) Distribution fromPoints A to E in (a).The time is 17 min

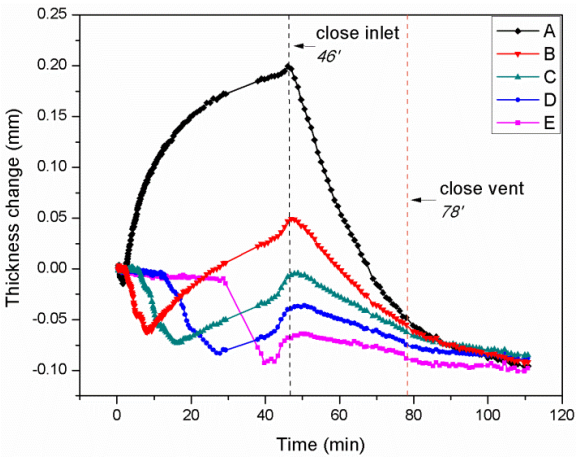

Fig. 5 Thickness evolution curves for Points A to E

Our explanation on the shrinkage stage is that the first contact of resin reduces the friction between fibers, making the stack much easier to be compacted. Additionally, the surface tension of the resin increases the compacting pressure.

Consequently, the thickness begins to decrease. Then, after the resin exceeds the least amount required for full saturation, friction no longer decreases. As the increasing amount of resin shares more of the compacting pressure in the stack, the stack expands. Based on this analysis of the thickness evolution, the deep blue part in Fig. 4 (b) can be considered as the flow front. Figs. 4 (a) and (b) coincide with each other very well, indicating that our analysis is correct and the 3D DIC system is valid.

IV. Distribution of Fiber Volume Fraction

A. Experiment

1. Material and Specimen

Fiber volume fraction is one of the most important parameters of composites. As we all know the carbon fiber and the resin have totally different coefficients of thermal expansion (CTE). Different fiber volume fractions may cause different coefficient of thermal expansion values. This experiment tried to estimate the distribution of the fiber volume fraction by testing the areal coefficient of thermal expansion.

A CFRP plate manufactured from VARTM process was used. The thickness is around 2 mm. In this VARTM process, a metal plate was used to make the up surface of the CFRP plate smooth, making it possible to measure the thickness relatively accurate [25]. The CFRP plate is about 290 mm long as shown in Fig. 6. Rectangular specimens were cut from the plate for the test of the coefficient of thermal expansion. The inlet and the vent indicate the infusion direction in the VARTM process. The specimen is about 14 mm wide and 42 mm long.

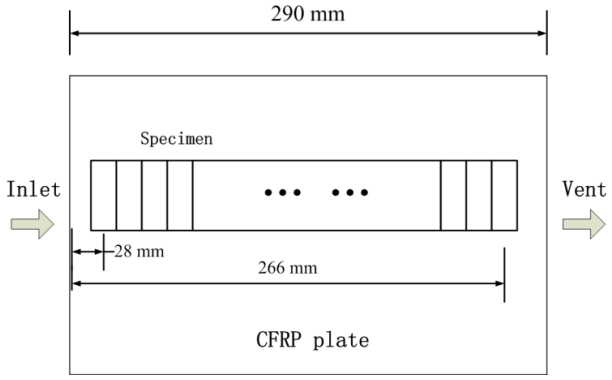

Fig. 6 Location of specimens

2. Test of CTE

The sketch of the setup for testing the coefficient of thermal expansion is shown in Fig. 7. The specimens were laid on a heater and covered by a transparent glass plate. A smooth plastic plate was put in between of the specimen and the heater to reduce the friction of their interface. The transparent glass plate was used to press the specimen to prevent the warp deformation of the specimens. The up surfaces of the specimens were painted with random patterns to perform DIC test. The camera took the pictures of the specimens before and after heating the specimens. The room temperature was 13°C and the target temperature of the specimens was set at 30°C.

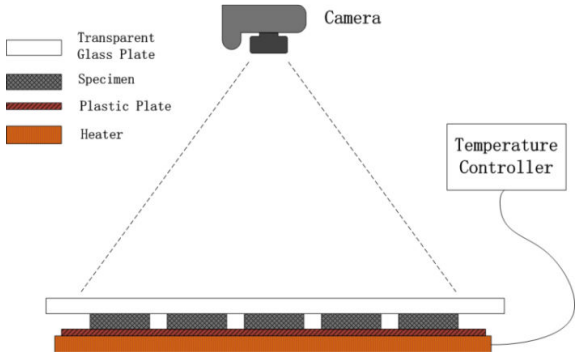

Fig. 7 Setup for test of CTE

For each specimen, the displacements of 2201 points which uniformly located on the specimen surface were tested through 2D-DIC technique. Strain is the displacement derivation of the position as defined as the follows

$$\varepsilon_x = \frac{\partial \delta_x}{\partial x}$$
$$\varepsilon_y = \frac{\partial \delta_y}{\partial y} \quad (3)$$

where ε_x and ε_y are the strain in x and y directions, respectively. δ_x and δ_y are the displacement in x and y directions, respectively. One of the simplest methods to calculate the strain from the displacement results is the finite difference method. However, this method usually leads to a large error due to some fluctuant results. In order to get an accurate result of the strain of a point, quadric surface equations were adopted to fit the displacement results of its vicinity area as follows

$$\delta_x = a_0 + a_1 x + a_2 x^2 + a_3 xy + a_4 y + a_5 y^2$$
$$\delta_y = b_0 + b_1 x + b_2 x^2 + b_3 xy + b_4 y + b_5 y^2 \quad (4)$$

The parameters, a_i and b_i (i=1,2, •••, 5), could be fixed through the least square procedure with the displacement results of the target point and its ambient points as shown in Fig. 8. Combining (3) and (4), the strain could be calculated through the following equation

$$\varepsilon_x = a_1 + 2a_2 x + a_3 y$$
$$\varepsilon_y = b_3 x + b_4 + 2b_5 y \quad (5)$$

The areal strain can be considered as the sum of ε_x and ε_y,

$$\varepsilon = \varepsilon_x + \varepsilon_y \quad (6)$$

Then, the coefficient of thermal expansion of a specimen is

$$CTE = \frac{\varepsilon_{ave}}{\Delta T}, \quad (7)$$

where ε_{ave} is the average areal strain of all the points on the

specimen.

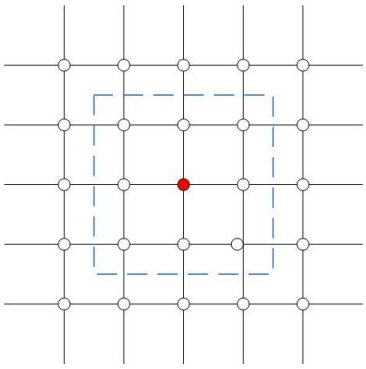

Fig. 8 Illustration for the calculation of strain

3. Calculation of Fiber Volume Fraction

The fiber volume fraction of the specimens were calculated roughly using the following equation

$$f_{fiber} = \frac{n \cdot \rho_f^s}{\rho_f^V \cdot h}, \quad (7)$$

where n is the number of fabric layers, ρ_f^s and ρ_f^V are the areal and volume density of the fabric, respectively. h is the thickness of samples, determined by a micrometer.

B. Results and Discussion

Fig. 9 shows the results of the coefficient of thermal expansion and fiber volume fraction. The lateral axis shows the distance of the specimen from the edge of the CFRP plate near the inlet to its location on the plate, as shown in Fig. 6. In order to emphasis the relationship between the coefficient of thermal expansion and the fiber volume fraction, the scale of fiber volume fraction in the graph is inverse, from 56.3 to 53.8. This graph shows that from the inlet to the vent the CFRP plate has increasing distribution of the fiber volume fraction. And the specimens near the inlet show a higher coefficient of thermal expansion. In order to ensure the reliability of the experiment, the test of the coefficient of thermal expansion was repeated three times. The results are shown Fig. 10. Though the results of each specimen are a little different, the three tests show the same distribution, indicating that the tendency is reliable.

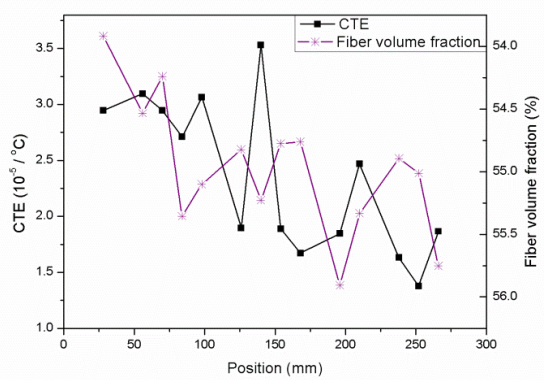

Fig. 9 Results of CTE and fiber volume fraction

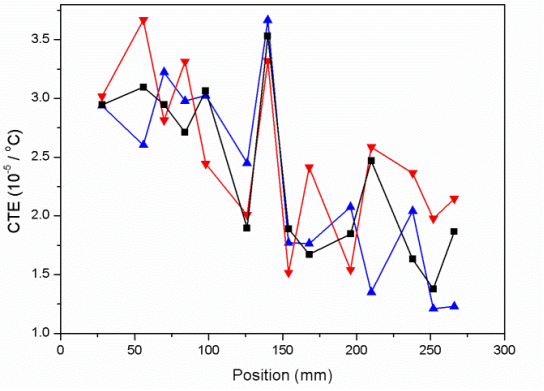

Fig. 10 Collection of results tested in three experiments

The distribution of the fiber volume fraction in Fig. 9 is reasonable, because a few of concentrations of the resin in the vicinity of the inlet in the resin infusion stage of VARTM process usually make the part near the inlet remain more resin, leading to a larger thickness. The order of the coefficient of thermal expansion of resin is 10^{-5}. The coefficient of fibers is even a little lower than 10^{-6} / °C. When a CFRP specimen is heated, the component of the resin should expand faster than the fibers do. The small expansion and the high tensile modulus of the fiber will restrict the expansion of the resin. When the fiber content is higher, this restriction will be stronger. Consequently, a specimen with a higher coefficient of thermal expansion should have a lower fiber volume fraction, coinciding with the relationship shown in Fig. 9. Additionally, from Fig. 9 we can find the coefficient of thermal expansion is sensitive to the fiber volume fraction. From the inlet to the vent, the fiber volume fraction only increases by about 3%, however the coefficient of thermal expansion decreases by near 50%, indicating a high sensitivity of this method.

V. Conclusion

In this paper, we did some trials on using digital image correlation method to monitor the resin infusion stage in VARTM process and estimate the fiber volume fraction distribution of a VARTM produced CFRP plate. The conclusions can be summarized as two points.

1. 3D-DIC technique is valid on monitoring the resin infusion stage in VARTM process. The results tested by 3D-DIC method are useful to analysis the regular of the flow of the resin.
2. Though we did not give an accurate relationship between the coefficient of thermal expansion and the fiber volume fraction of the CFRP material, it was proved that measurement of the coefficient of thermal expansion using 2D-DIC technique is a promising method to estimate the fiber volume fraction nondestructively.

ACKNOWLEDGMENT

This work was partly supported by a research grant from the Japan Society for Promotion of Science (#23656605), and by the Collaborative Research Program of Research Institute for Applied Mechanics, Kyushu University. The authors also would like to acknowledge SAERTEX GmbH & Co. KG and NAGASE & Co., LTD. for their support of the carbon fabric and the epoxy resin respectively.

REFERENCES

[1] Takeda F, Nishiyama S, Hayashi K, Komori Y, Suga Y, Asahara N. Research in the application of the VaRTM technique to the fabrication of primary aircraft composite structures. Tech Rev Mitsubishi Heavy Ind. 2005;42(5):1-6.
[2] Bender D, Schuster J, Heider D. Flow rate control during vacuum-assisted resin transfer molding (VARTM) processing. Composites Science and Technology. 2006;66(13):2265-2271.
[3] Johnson RJ, Pitchumani R. Enhancement of flow in VARTM using localized induction heating. Composites Science and Technology. 2003; 63(15):2201-2215.
[4] Johnson RJ, Pitchumani R. Flow control using localized induction heating in a VARTM process. Composites Science and Technology. 2007; 67(3-4):669-684.
[5] Alms JB, Glancey JL, Advani SG. Mechanical properties of composite structures fabricated with the vacuum induced preform relaxation process. Composite Structures. 2010;92(12):2811-2816.
[6] Nalla AR, Fuqua M, Glancey J, Lelievre B. A multi-segment injection line and real-time adaptive, model-based controller for vacuum assisted resin transfer molding. Composites Part A: Applied Science and Manufacturing. 2007;38(3):1058-1069.
[7] Kedari VR, Farah BI, Hsiao K-T. Effects of vacuum pressure, inlet pressure, and mold temperature on the void content, volume fraction of polyester/e-glass fiber composites manufactured with VARTM process. Journal of Composite Materials. 2011;45(26):2727-2742.
[8] Correia NC, Robitaille F, Long AC, Rudd CD, Šimáček P, Advani SG. Analysis of the vacuum infusion moulding process: I. Analytical formulation. Composites Part A: Applied Science and Manufacturing. 2005; 36(12):1645-1656.
[9] Simacek P, Advani SG. Modeling resin flow and fiber tow saturation induced by distribution media collapse in VARTM. Composites Science and Technology. 2007;67(13):2757-2769.
[10] Simacek P, Heider D, Gillespie Jr JW, Advani S. Post-filling flow in vacuum assisted resin transfer molding processes: Theoretical analysis. Composites Part A: Applied Science and Manufacturing. 2009; 40(6–7):913-924.
[11] Simacek P, Eksik Ö, Heider D, Gillespie Jr JW, Advani S. Experimental validation of post-filling flow in vacuum assisted resin transfer molding processes. Composites Part A: Applied Science and Manufacturing. 2012; 43(3):370-380.
[12] Govignon Q, Bickerton S, Kelly PA. Simulation of the reinforcement compaction and resin flow during the complete resin infusion process. Composites Part A: Applied Science and Manufacturing. 2010; 41(1):45-57.
[13] Govignon Q, Bickerton S, Morris J, Kelly PA. Full field monitoring of the resin flow and laminate properties during the resin infusion process. Composites Part A: Applied Science and Manufacturing. 2008; 39(9):1412-1426.
[14] Govignon Q, Bickerton S, Kelly P. Experimental investigation into the post-filling stage of the resin infusion process. Journal of Composite Materials. 2013;47(12):1479-1492.
[15] ASTM Standard D3171, "Standard Test Methods for Constituent Content of Composite Materials", ASTM International, West Conshohocken, PA, 2011.
[16] ASTM Standard D3529M, "Standard Test Method for Matrix Solids Content and Matrix Content of Composite Prepreg", ASTM International, West Conshohocken, PA, 2010.
[17] ASTM Standard D2584, "Standard Test Method for Ignition Loss of Cured Reinforced Resins", ASTM International, West Conshohocken, PA, 2011.
[18] Sutton M, McNeill S, Helm J, Chao Y. Advances in Two-Dimensional and Three-Dimensional Computer Vision. In: Rastogi P, editor. Photomechanics, vol. 77: Springer Berlin Heidelberg; 2000. p. 323-372.
[19] Uchino M. Sub-micron displacement measurement using a digital image correlation method. ATEM, Nagoya, Japan: The Japan Society of Mechanical Engineers; 2003. p. No.03-207.
[20] Uchino M, Yamaguchi T. 3-Dimensional Deformation Measurement Using Digital Image Correlation Method. JSEM 2006 Annual Conference on Experimental Mechanics, vol. 6 Kasugai, Japan: The Japanese Society for Experimental Mechanics; 2006. p. 77-80.
[21] Uchino M, Yamaguchi T. 3D deformation Measurement using Digital Image Correlation Method. the 2005 Annual Meeting of the JSME/MMD, vol. 5 Fukuoka, Japan: The Japan Society of Mechanical Engineers; 2005. p. 357-358.
[22] Yenilmez B, Sozer EM. Compaction of e-glass fabric preforms in the Vacuum Infusion Process, A: Characterization experiments. Composites Part A: Applied Science and Manufacturing. 2009;40(4):499-510.
[23] Yenilmez B, Sozer EM. Compaction of e-glass fabric preforms in the vacuum infusion process: (a) use of characterization database in a model and (b) experiments. Journal of Composite Materials. 2013; 47(16):1959-1975.
[24] Yang JS, Xiao JY, Zeng JC, Jiang DZ, Peng CY. Compaction Behavior and Part Thickness Variation in Vacuum Infusion Molding Process. Appl Compos Mater. 2012;19(3-4):443-458.
[25] Chen D, Arakawa K. Flexural Properties of VARTM Manufactured CFRP Plate. 9th International Conference on Fracture & Strength of Solids Jeju2013. p. 116.